LBL-16269
c.2

Lawrence Berkeley Laboratory

UNIVERSITY OF CALIFORNIA

RECEIVED
LAWRENCE
BERKELEY LABORATORY
FEB 1 1984
LIBRARY AND
DOCUMENTS SECTION

EARTH SCIENCES DIVISION

Presented at the Society of Petroleum Engineers
58th Annual Technical Conference and Exhibition,
San Francisco, CA, October 5-8, 1983

THERMAL EFFECTS OF REINJECTION IN GEOTHERMAL RESERVOIRS WITH MAJOR VERTICAL FRACTURES

K. Pruess and G.S. Bodvarsson

October 1983

TWO-WEEK LOAN COPY

This is a Library Circulating Copy which may be borrowed for two weeks. For a personal retention copy, call Tech. Info. Division, Ext. 6782.

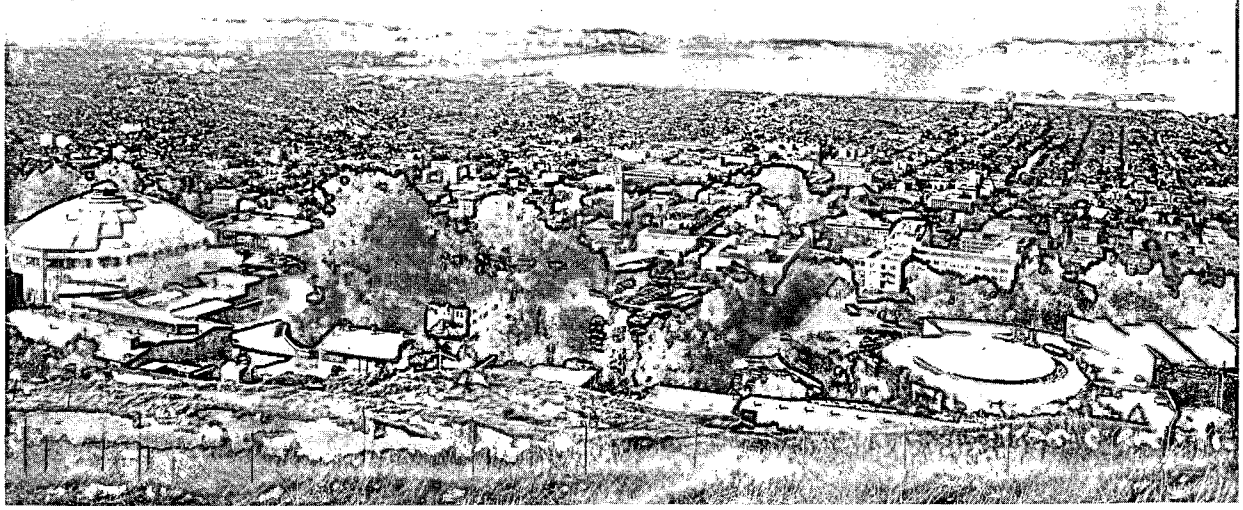

LBL-16269
c.2

Prepared for the U.S. Department of Energy under Contract DE-AC03-76SF00098

DISCLAIMER

This document was prepared as an account of work sponsored by the United States Government. While this document is believed to contain correct information, neither the United States Government nor any agency thereof, nor the Regents of the University of California, nor any of their employees, makes any warranty, express or implied, or assumes any legal responsibility for the accuracy, completeness, or usefulness of any information, apparatus, product, or process disclosed, or represents that its use would not infringe privately owned rights. Reference herein to any specific commercial product, process, or service by its trade name, trademark, manufacturer, or otherwise, does not necessarily constitute or imply its endorsement, recommendation, or favoring by the United States Government or any agency thereof, or the Regents of the University of California. The views and opinions of authors expressed herein do not necessarily state or reflect those of the United States Government or any agency thereof or the Regents of the University of California.

Presented at SPE 58th Annual Technical Conference and Exhibition, San Francisco, CA, October 5-8, 1983.

LBL-16269

THERMAL EFFECTS OF REINJECTION IN GEOTHERMAL RESERVOIRS WITH MAJOR VERTICAL FRACTURES

K. Pruess and G.S. Bodvarsson

Earth Sciences Division
Lawrence Berkeley Laboratory
University of California
Berkeley, California 94720

ABSTRACT

In many geothermal fields there is evidence for rapid migration of injected fluids along "preferential flow paths", presumably along fractures. The potential for unacceptable fluid temperature decline at production wells as a consequence of large scale injection is of obvious concern to geothermal developers, and methods are needed for evaluating the thermal response of "fast-paths" to injection. One difficulty encountered in analyzing test data is that the geometry of the flow path(s) may be speculative and ambiguous, leading to unreliable predictions of thermal interference. Fast pathways may often be provided by major vertical or nearly vertical fractures and faults with approximately linear flow geometry. This paper discusses possibilities for characterizing the thermal properties of fast paths by means of different types of tests (tracers, pressure transients, non-isothermal injection). Thermal breakthrough in vertical fractures is examined in some detail, using an idealized model for which an analytical solution is available. The model shows that rapid tracer returns are not necessarily indicative of rapid thermal interference. Thermal breakthrough predictions can be made from tracer data only, if both fluid residence time and tracer dispersion are taken into account. However, due to the geometric simplifications necessary in analyzing the tracer data, thermal interference estimates on this basis appear questionable. Pressure transient tests can provide additional parameters for thermal interference predictions, but they cannot resolve the problem of non-uniqueness. A more reliable determination of thermal characteristics of fast paths appears possible from non-isothermal injection tests, combined with numerical simulation. We employ a mixed numerical/semi-analytical approach to model the three-dimensional fluid and heat flow in injection-production systems in vertical fractures, with heat transfer to and from the adjacent rock matrix. Illustrative calculations of thermal recovery after different injection periods suggest that shutting-in an injection well can prevent unacceptable temperature declines at production wells.

References and illustrations at end of paper.

INTRODUCTION

Reinjection of spent geothermal brines is the most attractive method for their disposal. Field experience and theoretical work have shown that properly designed injection systems can avoid premature thermal interference at production wells, and may serve additional purposes, such as maintenance of reservoir pressures, and enhancement of ultimate energy recovery. There has been some controversy in the literature regarding benefits and drawbacks of reinjection. At the present time it seems clear that the issues are largely site-specific, and that reservoir response to reinjection is strongly dependent upon formation properties and the thermodynamic state of the reservoir fluids. Whether or not reinjection at a given site is deemed desirable from the standpoint of reservoir management, it appears that for environmental reasons most future geothermal projects will require full reinjection as a method of waste disposal. There is a need for methods of designing and testing reinjection systems such as to avoid premature breakthrough of colder fluids at the production wells.

An advisory panel convened by the U.S. Department of Energy identified the development of techniques for monitoring, prediction, and control of the migration of injected waters as an urgent priority. Depending upon the geological characteristics of a geothermal reservoir, this can be a rather difficult task. For reservoirs approaching the idealization of a porous medium of uniform thickness, porosity, and permeability, analytical solutions are available for estimating the migration of thermal (cold) fronts away from injection wells (Lauwerier, 1955; Bodvarsson, 1972; Gringarten and Sauty, 1975; Hanson and Kasameyer, 1978). However, most high-temperature geothermal reservoirs are situated in fractured volcanic rocks. There is plenty of field evidence showing that in fractured reservoirs injected water can migrate rather rapidly

to production wells. The possibility of rapid thermal breakthrough along "preferential pathways" is of obvious concern to field developers.

In the next section we review some field evidence for "fast paths", and discuss possibilities and limitations for determining the thermal characteristics of fast paths by non-thermal means. We present idealized models of fast paths, and examine their applicability to field situations. It is emphasized that tracer tests and pressure transient tests can only provide incomplete and ambiguous information on the thermal characteristics of fast paths. More reliable predictions of thermal interference are possible from non-isothermal injection tests. Numerical simulations incorporating approximate analytical solutions are then used to examine thermal breakthrough and recovery in vertical fractures.

"FAST PATHS"

Rapid migration of injected waters to production wells has been observed in many geothermal fields by means of (natural or artificial) tracers, and enthalpy transients. Table I summarizes some of the pertinent data. Tracer migration velocities of 0.1 to 100 m/hr, over distances of several hundred meters, provide clear evidence for preferential pathways, presumably along fractures. For comparison, consider average linear velocities in a porous medium-type reservoir, $v = q_v/\pi H\phi r$. Inserting representative values ($q_v = 0.02$ m^3/s, $H = 200$ m, $\phi = 10\%$, $r = 300$ m) results in $v = 3.8 \times 10^{-3}$ m/hr, which is several orders of magnitude lower than tracer velocities observed in many fractured reservoirs.

It should be emphasized that rapid tracer returns alone do not indicate possible or actual problem situations. As far as field management is concerned, the important parameter is velocity of the thermal front. This depends on various characteristics of the preferential pathway(s), which are only partially determined by the speed of tracer movement. Indeed, tracer breakthrough time is essentially a measure of the total volume of the preferential path between injection and production wells (see equation 14, below). Thermal migration on the other hand is largely determined by the total available surface area for heat transfer from the reservoir rocks to the preferential flow path. From an analysis of tracer dispersion one can obtain an estimate of the effective fracture aperture (Fossum and Horne, 1982). This, together with data on fracture volume between injection and production points, permits an approximate estimate of total fracture surface area. This estimate, however, depends on hypothetical assumptions about the geometry of the preferential flow path, so that predictions of thermal interference on this basis are questionable.

Several authors have proposed injection of "reactive" tracers, which would in some way interact with the wall rocks and thus permit an estimate of heat transfer area (e.g. Robinson, 1982). Although this approach holds some promise, it is unlikely that the ambiguities regarding heat transfer can be resolved. Fracture faces may have considerable roughness, which would cause effective heat transfer areas to be overestimated on the basis of reactive tracer data. Further complications arise from the presence of dead end pores, diffusion into which would also tend to diminish the return of tracer, causing unrealistically high estimates of heat transfer area (Coats and Smith, 1964). Preferential flow paths may be contorted, causing thermal interference between different path segments, which could not be predicted from tracer tests (Zyvoloski, 1981). Due to thermal drawdown over extended injection periods, the flow field may change with time, chiefly from buoyancy and viscosity effects. This cannot be predicted on the basis of tracer data obtained over relatively short flow periods. To summarize, it appears that even if rather ideal reactive tracers were available, the possible inference regarding the thermal characteristics of fast paths would remain seriously incomplete. The uncertainties tend to be non-conservative, i.e., thermal breakthrough could occur more rapidly than might be estimated from tracer returns.

Additional information on the nature of fast paths can be obtained from enthalpy transients (observed e.g. in Krafla, Iceland; Bodvarsson et al., 1983), and pressure transients. It should be stressed, however, that interpretation of field test data invariably requires certain model assumptions and approximations, which will lead to uncertainties in heat transfer predictions. Thermal retardation is very strongly affected by matrix-fracture interaction, which may have quite different and probably often much smaller impact on migration of injected water and tracer, and on pressure diffusion. One should not expect that the processes and parameters governing heat transfer could be unambiguously resolved by non-thermal tests, as these involve different physical processes, and probe different properties of the flow system. The only type of test which can provide reliable estimates of the heat transfer properties of preferential pathways appears to be a thermal interference test. This has been carried out successfully in small experimental hot dry rock reservoirs (Murphy and Tester, 1979; Zyvoloski, 1981; Dash et al., 1981; Murphy et al., 1981). For conditions of interest in natural hydrothermal systems, however, thermal interference tests cannot be carried out ahead of a long-term injection program, as required test durations may be many years. In order to make a reliable determination of the thermal characteristics of preferential pathways, it is necessary to implement a trial injection program on a substantial scale.

If no thermal drawdown data are available, thermal interference analysis must be based in part on hypothetical model assumptions, which are made on the basis of geological, geophysical, or geochemical information about a geothermal field, and on the basis of mathematical convenience. The element of uncertainty inherent in this type of approach requires a conservative philosophy in injection design, with considerable safety margins against premature thermal breakthrough.

SOME IDEALIZED MODELS

Useful insight into thermal interference can be obtained from idealized models of preferential pathways, including horizontal fractures, vertical

fractures, and pipes. High-permeability horizontal zones are common in volcanic rocks, especially at the contacts between lava flows (Bodvarsson, 1975). This type of permeable zone has been identified in several geothermal fields; e.g. Baca, New Mexico (Grant and Garg, 1981), Ohaaki, New Zealand (Grant, personal communication, 1983); and various geothermal fields in Iceland (Fridleifsson, 1975). Bodvarsson and Tsang (1982) studied the case of injection into horizontal permeable zones (fractures). Their analysis indicated that a porous medium-type situation with uniform thermal sweep is attained at surprisingly small distances from the injection well. This favorable result is in part due to the radial flow geometry of horizontal zones. For radial flow systems, the flow velocity is proportional to 1/r and the surface area for heat transfer grows proportional to r^2. Consequently, the retardation of the thermal front due to heat conduction from the rock matrix is strong. For cases where horizontal permeable zones are dominant, the formulas given by Bodvarsson and Tsang (1982) can be used to estimate proper locations of injection wells.

However, nearly vertical fractures, faults, and dikes are also commonly encountered in geothermal systems. These structures could conceivably offer thermally short-circuiting pathways with linear flow geometry. We shall here review some simple analytical results for temperature fields in vertical fractures. Subsequently, we shall examine possible generalizations to other flow channel geometries.

VERTICAL FRACTURES

In order to develop an analytically solvable model, idealizations or approximations must be made for (i) the fracture geometry, (ii) the initial and boundary conditions, and (iii) the fluid and heat flow fields in fracture and wallrocks, respectively. Consider a vertical fracture of aperture w and porosity ϕ_f, embedded in impermeable rock of uniform thermal properties, and infinite lateral extent. Initially the entire system has a uniform temperature T_o, and at time t = 0 water of temperature T_{in} is injected into the fracture at a constant pore velocity v_w. It is assumed that water flows only horizontally, with pore velocity equal to v_w throughout the fracture at all times. At a distance x from the injection point, the mean arrival time (residence time) of non-reactive tracer is $t_b = x/v_w$. The thermal front is retarded in comparison to the tracer by two different mechanisms, namely, thermal equilibration within the fracture, and lateral heat conduction from the reservoir rocks across the fracture faces. Neglecting heat conduction in the direction of water flow, the water temperature in the fracture can be computed from a solution obtained by Lauwerier (1955) for non-isothermal injection into a horizontal layer:

$$T(x,t) = T_o + (T_{in} - T_o)\ \mathrm{erfc}\ (\zeta(x,t)) \cdot U(t-t^*) \tag{1}$$

The argument of the complementary error function is

$$\zeta(x,t) = \frac{\sqrt{\lambda_2\rho_2c_2}\ \ x}{w\phi_f\rho_w c_w v_w\ \sqrt{t - t^*}}$$

$$= \frac{\sqrt{\lambda_2\rho_2c_2}\ \ x}{c_w(q/H)\ \sqrt{t - t^*}} \tag{2}$$

where $q/H = w\phi_f\rho_w v_w$ is the mass injection rate per unit fracture height, and U is the Heaviside step function

$$U(y) = \begin{cases} 1 \text{ for } y > 0 \\ 0 \text{ for } y < 0 \end{cases} \tag{3}$$

Here, t* is the breakthrough time of the thermal front in the absence of lateral heat conduction, and is given by (Bodvarsson, 1972)

$$t^* = \frac{\rho_1 c_1 x}{\rho_w c_w \phi_f v_w} \tag{4}$$

In the absence of lateral heat conduction, the temperature at the front jumps from T_o to T_{in}. The lateral heat conduction causes the temperature profile to diffuse, and in general the thermal front may be defined as the locus of points where temperature has dropped to a certain fraction of the initial difference between reservoir and injection temperature:

$$T_f = T_{in} + f(T_o - T_{in}) \tag{5}$$

For a symmetrical front one could chose f = 0.5 to define the front. However, in the present problem fronts are highly non-symmetrical, and a smaller temperature decline is very significant in many geothermal applications. A value of f = 0.75 may be a more useful measure of the thermal front. From the above definition, the front location is given by

$$\mathrm{erfc}\ (\zeta_f) = 1 - f \tag{6}$$

For f = 0.75 we have $\zeta_f = 0.81342$.

THERMAL BREAKTHROUGH

From equations (2) and (6), the thermal breakthrough time t_f at a distance x_f from the injection point can be written as

$$t_f = t^* + \frac{\alpha}{\zeta_f^2}\ \frac{x_f^2}{(q/H)^2} \tag{7}$$

Here $\alpha = \lambda_2\rho_2c_2/c_w^2$ is a group of thermal parameters which is not strongly dependent upon site-specific conditions.

The first term in equation (7) can be re-written in terms of mean tracer arrival (or fluid residence) time t_b

$$t^* = \frac{\rho_1\ c_1}{\rho_w\ c_w}\ \frac{t_b}{\phi_f} \tag{8}$$

This first term represents the thermal breakthrough time in the absence of lateral heat conduction, whereas the second term represents the thermal retardation from lateral heat conduction alone. It is interesting to note that both effects are additive in their impact on thermal breakthrough time. Many of the parameters in equations (7) and (8) depend little on temperature or site-specific conditions, which permits some general conclusions to be made. With tracer velocities in fractured geothermal reservoirs being typically of the order of 1m/hr, a typical tracer breakthrough time at an observation well distance of 250 m is of the order of 10 days. Thermal retardation from equilibration within the fracture, t^*/t_b, is unlikely to exceed 10 in practical cases (see equation 8), so that thermal breakthrough in the absence of lateral heat conduction will occur in a matter of months. Obviously, lateral heat conduction must be relied upon for providing thermal breakthrough times commensurate with the typical design life of geothermal power installations (30 years).

Equation (7) gives an expression for partial thermal breakthrough time from lateral heat conduction as a function of x_f and q/H (second term in equation 7), which appears to be of rather limited utility. The rate of injection into a preferential flow path may be estimated in the field from total injection rate q_o and fractional cumulative recovery of tracer τ, $q \approx \tau \cdot q_o$, but meaningful estimates of fracture height H may be impossible.

A more useful expression can be obtained by introducing fluid residence time t_b:

$$t_{f2} = \frac{\alpha}{\rho_w^2 \zeta_f^2} \frac{t_b^2}{\phi_f^2 w^2} \tag{9}$$

This relationship is plotted in Figure 1 for a thermal front parameter f = 0.75 (corresponding to ζ_f = 0.81342). The parameter t_b can be directly obtained from field observation, and the group $\phi_f w$ can be determined from an analysis of tracer dispersion (Horne and Rodriguez, 1981; Fossum and Horne, 1982). Horne and coworkers have proposed a model of linear flow in a fracture, in which the observed tracer dispersion is caused by an interplay of molecular diffusion with a parabolic velocity profile across the fracture width. Based on their model, the effective fracture aperture can be expressed as

$$\phi_f w = \sqrt{\frac{210\ D}{N_{Pe}}\ t_b} \tag{10}$$

On the basis of their linear flow dispersion model, Fossum and Horne (1982) were able to obtain good matches for tracer return data at Wairakei geothermal field. Their analysis provides some justification for the underlying model, and it provides estimates of the parameters t_b and N_{Pe}. A thermal breakthrough prediction can then be made from equations (9) and (10), utilizing only reservoir parameters obtained from tracer tests. However, tracer data can usually be described with a variety of different models and assumptions, so that the reliability of fracture aperture estimates from a dispersion analysis is uncertain.

The assumption of linear one-dimensional flow, which is implicit in the tracer analysis of Fossum and Horne, can be tested by means of thermal interference tests. In this way a more reliable prediction of thermal drawdown may be achieved. We sugggest the following procedure. Monitoring production temperatures during an injection experiment, one can obtain the quantity

$$\zeta = \mathrm{erfc}^{-1}\left(\frac{T_o - T}{T_o - T_{in}}\right) \tag{11}$$

as a function of time. If ζ is plotted versus time on log-log paper, a straight line with slope -1/2 should result if flow is in fact linear along a planar fracture (see equation 2; the term t* is usually insignificant in comparison to t, except at very early times). If the half-slope is observed, the plot can be used to estimate future production temperatures by extrapolation. From a pair of values (t, ζ(t)) one can compute the parameter $\phi_f w$, or q/H. Estimating q on the basis of fractional recovery of tracer, it is also possible to obtain the effective fracture surface area S = 2Hx.

MORE GENERAL FLOW CHANNELS

The discussion so far was limited to one-dimensional linear flow. The function $\zeta(x,t)$ given in equation (2) can be rewritten in a number of ways, which are instructive in showing the dependence of thermal front migration upon the geometric parameters of the flow channel. Introducing the fracture surface area S = 2Hx between the injection point and an observation point at distance x, we have

$$\zeta(S,t) = \frac{\sqrt{\lambda_2 \rho_2 c_2}\ S}{2\ q\ c_w \sqrt{t-t^*}} \tag{12}$$

The thermal breakthrough time in the absence of lateral heat conduction, Equation (4), can also be re-written in terms of total volume V = wHx and flow rate q of the preferential flow path

$$t^* = \frac{\rho_1\ c_1\ V}{c_w\ q} \tag{13}$$

Equations (12) and (13) are written in terms of parameters S, V, and q, which have meaning for any type (geometry) of flow channel, not just for vertical fractures. This is suggestive of a greater range of validity of Lauwerier's solution than was implied in the restrictive approximations made in the derivation of equations (1) and (2). Indeed, it was shown by Gringarten and Sauty (1975) that Lauwerier's solution is applicable to the steady, nonisothermal flow field of an injection-production doublet in a horizontal aquifer of uniform thickness. When reformulating Lauwerier's heat balance equations for flow channels of more general geometry, it is apparent that Lauwerier's solution is valid as long as the surface-to-volume ratio S/V in a flow channel is constant, independent

of position. This requirement is obviously fulfilled for all stream channels in a production-injection doublet in a horizontal aquifer of uniform thickness h, as considered by Gringarten and Sauty, where $S/V = h/2$. Equations (1) and (12) are identical to Gringarten and Sauty's solution for any particular stream channel in the doublet problem with horizontal flow.

A further generalization for applications is gained by rewriting equation (2) or (12) in terms of fluid residence time, as suggested by Hanson and Kasameyer (1978). Noting that the total reservoir volume swept by injection is

$$V = \frac{q t_b}{\phi_f \rho_w} \tag{14}$$

we have

$$\zeta = \frac{\sqrt{\lambda_2 \rho_2 c_2}\,(S/V)\, t_b}{2\, \phi_f \rho_w c_w \sqrt{t-t^*}} \tag{15}$$

While the parameters entering equations (12) through (15) can be defined for very general flow channel geometry, the validity of these equations is restricted to flow channels with constant surface-to-volume ratio S/V throughout. It should be emphasized that all of the various forms given for ζ (equations 2, 12, 15) contain certain geometrical parameters (w, ϕ_f, q/H, q/S, S/V) which are rather elusive in practical field situations, unless actual thermal interference tests can be made. Therefore, the practical utility of the analytical model appears limited.

In practical circumstances, quantitative matching and prediction of thermal interference will often require a detailed numerical modeling effort (Murphy et al., 1981). This is necessitated not only by the geometrical complexity of fracture systems, but also by operating conditions that involve time-varying flow rates, and non-uniform initial temperatures.

It is interesting to compare thermal breakthrough in horizontal and vertical fractures of identical aperture w and porosity ϕ_f. Based on the foregoing discussion, an observation well placed at a distance x from the injection well will "see" the same thermal history in either case if the swept surface areas are identical (assuming pure radial flow in the horizontal fracture, and one-dimensional horizontal flow in the vertical fracture). The condition for identical thermal history can be written

$$H = \pi x \tag{16}$$

For $x < H/\pi$, thermal interference will be more rapid in the radial flow geometry, while for $x > H/\pi$ it will be more rapid in the linear flow geometry.

FIELD EXAMPLE

To illustrate the simple thermal analysis proposed above (discussion following equation 11) we present an application to "run segment 2" of the Fenton Hill hot dry rock experiment (Murphy and Tester, 1979; Dash et al., 1981; Murphy et al., 1981). In this experiment, fresh water at 25°C was injected continuously for a period of 75 days into a man-made geothermal reservoir. After passing through a fracture system at about 2.8 km depth, the water was retrieved at a production well where its temperature was monitored. From the temperature data given in the above references, we calculate the parameter ζ from equation (11). This is plotted against time on log-log paper in Figure 2. Two cases were considered. Assuming an injection temperature of 65°C, which is the downhole temperature in the injection well (Dash et al., 1981), we obtain a set of points which do not fall on a straight line with a half-slope. When injection temperature is set equal to the well head temperature of 25°C, the resulting data points are well matched by a straight line of slope -1/2. This indicates that the entire heat transmission system, including injection wellbore and fractures, approximates the behavior of a linear flow system in a planar fracture. This holds only approximately, because neither flow rate nor initial reservoir temperature were constant in this experiment. Utilizing the data given by Murphy and Tester (1979), and Dash et al. (1981), the value $\zeta = 0.443$ at $t = 50$ days (see Figure 2) yields a total heat transfer area of 26,800 m^2. This value includes effects from wellbore heat transmission, and it is compatible with values of 16,000 - 30,000 m^2 (for both fracture faces) obtained by Dash et al. (1981) through detailed heat transfer modeling.

We now turn to a consideration of fracture apertures. During the above mentioned heat extraction experiment several tracer tests were run. Tester, Bivins, and Potter (1982) developed two-dimensional type curve matches to the tracer data, which when combined with the fracture area obtained from heat transfer modeling, yield an estimated effective fracture aperture of $\phi_f w = 5 - 5.8$ mm. We use their published data for tracer test 1-3 ($t_b = 1633$ s; $N_{Pe} = 1.06$), and apply the method of Fossum and Horne to obtain an independent estimate of effective fracture aperture based solely on tracer data, equation (10). Assuming a value of $D = 10^{-10}$ m^2/s for molecular diffusivity, as recommended by Fossum and Horne, equation (10) yields $\phi_f w = 5.7$ mm. This agrees very closely with the values obtained by Tester et al. (1982), which in view of the different assumptions made in their analysis is probably somewhat fortuitous. Nonetheless it may indicate that parameters obtained from tracer tests alone may be useful for thermal interference predictions in preferential flow paths.

PERMEABLE ROCK MATRIX

If the rock matrix is permeable thermal interference along a preferential flow path will be retarded, because the rate of fluid flow in the fast path will diminish with distance from the injection point, due to leakage into the rock. This effect is here considered for the cases of a single vertical or horizontal fracture, embedded in permeable rock. We assume injection at constant rate, one-dimensional (linear or radial) flow in the fracture, and one-dimensional flow in the rock matrix perpendicular to the fracture faces. With

these approximations, solutions for the flow rate in the fracture as a function of distance from the injection point can be obtained in closed analytical form (in the Laplace domain; see the Appendix).

Figure 3 shows the fractional flow rate along the fractures as a function of a parameter ξ, which is a combination of distance from the well (x or r), time, and various fracture and rock properties, $\xi = x(k_r C_r \phi_r \mu / k_f^2 w^2 t)^{1/4}$. This parameter was chosen because it allows all cases to be represented by a single curve. The parameter shows that the dimensionless flow rate along the fracture is dependent upon $x/t^{1/4}$, and more strongly dependent upon the fracture parameters ($\sqrt{k_f w}$) than the rock matrix parameters ($(\phi_r C_r k_r)^{1/4}$). It also depends upon the fluid viscosity, as the pressure buildup in the fracture is directly related to the viscosity.

Figure 3 shows that there is relatively more leakage for the vertical fracture case than the horizontal fracture one. This result is somewhat surprising in view of the large surface area for fracture/rock matrix interflow in the case of horizontal fractures. However, the dominating factor is the pressure buildup in the fractures. In the horizontal fracture case the pressure drop along the fracture depends upon the logarithm of distance, whereas in the vertical fracture case the pressure drop is linear with distance. Consequently, the pressure buildup in the vertical fracture case is larger except very close to the well, and more fluids are forced into the rock matrix.

Table 2 illustrates the fluid leakage into the rock matrix in terms of real parameters. The table gives the fractional flow rate along the fracture for various values of distance (r or x), and parameters $k_f w$ and k_r. The table shows that fluid leakage to the rock matrix will typically be less than 10% except for the case of rather small $k_f w$ and large k_r. As one would expect that for a fast path $k_f w$ is significantly larger than 10^{-14}, the fluid leakage to the rock matrix will be negligible in many cases.

PRESSURE TRANSIENT ANALYSIS

In the above discussion we emphasized that predictions of thermal interference can only be made when a specific model of the preferential flow path has been established. Geologic evidence can help establish such a model. For example, major fractures or fault zones identified at the surface can suggest that the fast path connecting injection and production wells may be visualized as a vertical fracture. Similarly, the identification of permeable zones in wells at approximately the same depth may suggest a continuous horizontal permeable zone; in this case a horizontal fracture model may be appropriate. When an appropriate geometrical model of a fast path has been identified, we must attempt to quantify the important parameters that govern the response of the system to cold water migration.

Ideally, one would like to determine the fracture geometry (e.g., fracture aperture, w, and height, H) and hydraulic parameters (fracture porosity, ϕ_f, and permeability, k_f). Some parameter values may be obtained through use of pressure transient tests.

In order to analyze pressure transient data for the determination of geometric and hydraulic parameters, the rate of fluid flow into the fast path must be known. Tracer data show that generally only a small portion (typically 1-10%) of the fluids injected travel along the fast path to the observation point. The remainder flow along other fractures intercepting the injection well or in the rock matrix itself. For a well test conducted over the entire open interval of an injection well it is very difficult to determine the transient fraction of the injected fluids that enter the fast path.

If the feed point of the fast path in the injection well can be identified from well logs or spinner data, it may be possible to pack off a small zone containing that fracture zone. In this case all of the injected fluids would enter the fast path, and conventional methods of analysis developed in the petroleum and groundwater literature can be applied.

Various pressure transient solutions are available for wells intersecting single fractures. These have been summarized by Earlougher (1977) and Raghavan (1977). In general, these solutions show that the early time data can be used to deduce some of the fracture parameters needed. However, it is generally not possible to determine individual parameters but only groups such as wk_f, or $\phi_f k_f$, etc. These may provide important constraints for numerical modeling of thermal processes in fast paths, but it appears unlikely that pressure transient testing alone can determine the parameters needed for thermal breakthough calculations.

NUMERICAL SIMULATIONS

In this section we present some results of numerical simulations of fluid and heat flow in vertical fractures. The purpose of the numerical experiments is twofold: (i) to explore the significance of physical effects which were neglected in the analytical model, in particular effects of buoyancy, time-dependent flow fields, and hydrodynamic sweep efficiency; and (ii) to study temperature recovery at production and injection wells, when injection is stopped after significant temperature decline has occurred.

The latter point is of considerable practical importance. In the above discussion, we emphasized that estimates of thermal properties of preferential flow paths not based on thermal interference tests are probably unreliable, and can not provide conservative margins of safety on which to base injection design. Data from which future thermal interference may be predicted with confidence can only be obtained from pilot injection operations, with monitoring of production temperatures over a period of months or years. If data begin to show trends of thermal interference which are detrimental to production, it is of interest to know to what extent and over what time scale thermal degradation is reversible if the injection well causing the interference is shut in.

Migration of injected fluids in vertical fractures, with heat transfer from the wall rocks, is a three-dimensional problem. A "head-on"

numerical approach is computationally very intensive, and it is desirable to economize on the numerical work as much as possible, without compromising the physics of the problem to be studied.

The simulations reported here were carried out with the geothermal version of our general purpose simulator MULKOM (Pruess and Narasimhan, 1982; Pruess, 1983), into which we incorporated the semi-analytical method for lateral heat transfer by conduction, as developed by Vinsome and Westerveld (1980). This permits very efficient calculations for problems with impermeable rock matrix, effectively reducing the numerical work to that of a 2-D problem. To test the accuracy of the numerical method, we performed simulations of non-isothermal injection into a one-dimensional fracture. Figure 4 shows that the agreement with the analytical solution of Lauwerier (1955), Equations (1) and (2), is excellent. Vinsome and Westerveld demonstrated in their paper that their method gives accurate results also in cases with non-monotonic temperature variations at the rock faces.

A schematic diagram of the injection-production system considered is given in Figure 5, and Table III summarizes parameters used in the simulations. These parameters are intended to be representative of typical fast path conditions which may be encountered in liquid-dominated fractured geothermal reservoirs (see Table I). The choice of an injection rate of 4 kg/s into the fracture was based on a typical total injection rate of 40 kg/s per well, of which typically 10 percent may enter a preferential flow path, as inferred from cumulative tracer returns observed in the field (see Table I). The choice of effective fracture apertures $\phi_f w$ = 5-20 mm deserves comment. Apertures of this magnitude are consistent with estimates based on tracer returns and heat transfer data for the Fenton Hill hot dry rock reservoir (Tester et al., 1982) and for the Wairakei geothermal field in New Zealand (Fossum and Horne, 1982). Field evidence indicates that effective fracture aperture $\phi_f w$ and permeability k_f are essentially independent parameters, which are not related by the "cubic" law for idealized parallel-plate fractures (Witherspoon et al., 1980). "Real" fractures have considerable surface irregularities and roughness, and are partially filled with debris. The average parameters $\phi_f w$ and k_f of real fractures are primarily determined by their "wide" and "narrow" portions, respectively. Field data on tracer migration speeds and cumulative tracer returns from fractured geothermal reservoirs clearly show that fracture volumes are typically several orders of magnitude larger than would be expected if apertures were related to permeability by the "cubic law". For a fracture height of 200 m and an effective aperture of 20 mm, our injection rate of 4 kg/s corresponds to a realistic (large) speed of tracer migration of 5.0 m/hr. Permeabilities of preferential flow paths may typically be in the range of tens or hundreds of darcies. Fracture permeabilities of 50-500 darcies were chosen in our simulations because this gives a "reasonable" pressure buildup at the injection well of a few bars, and because this range covers the cases of "weak" and "strong" buoyancy effects (see below).

Results of our simulations are presented in Figures 6-14. In most cases the "upper" injection and production points (I and P in Figure 5) were used, and grid blocks of 20m x 20m were employed. Test calculations made with and without a gravity correction for flowing bottomhole pressure in the production wells gave virtually identical results for flow patterns and temperature contours in the fracture. Therefore, in subsequent calculations bottomhole pressure was specified as constant at its initial hydrostatic value, P_{wb} = 9.56 MPa. For a fracture height of H = 200 m, production temperatures are virtually independent of fracture permeability (Figure 6), which is surprising because flow patterns and thermal sweeps are rather different, see Figures 7-12. For the lowest permeability of 50 darcy, larger pressure gradients occur from injection so that the relative importance of gravity effects is diminished. Horizontal flow rates change little with time and show little variation over the height of the fracture (Figure 7). The temperature field after one year indicates a preferential sweep along the line connecting injection and production points (Figure 10). For higher permeability buoyancy effects are more pronounced, resulting in a loss of hydrodynamic sweep efficiency, as the upper portions of the fracture are increasingly bypassed by the injected water (Figures 8 and 9). This effect is offset by the increase in average thermal path length between injector and producer. It is interesting to note that the downward slumping of the injected plume diminishes with time in all cases so that sweep efficiency increases. This effect can be clearly seen when comparing production temperatures with those predicted from a 1-D uniform sweep model (Lauwerier solution; Figure 6). Initially the temperature drop in the 2-D cases is much more rapid, but the ratio $\Delta T(2\text{-}D)/\Delta T(1\text{-}D)$ diminishes with time. Lowering the injection point (to I' in Figure 5) has little effect, but lowering the production point (to P' in Figure 5) gives a more rapid temperature decline. This suggests that injection should not be made above the production horizon. Extending the fracture another 200 m downward, for a total height of 400 m, results in a strongly reduced thermal decline and an excellent nearly uniform sweep, see Figures 6 and 13. The temperature contours in Figure 13 are drawn for the case where injection and production points are at a height of 350 m, 50 m below the fracture top. Thermal degradation for the case H = 400 m, w = 1 cm is slower than in the cases with H = 200 m, w = 4 cm (see Figure 6), although average speed of tracer migration in the former case is larger by a factor of 2. This illustrates a point made above, namely, that tracer velocities do not necessarily correlate with thermal breakthrough times.

Figure 14 shows the temperature recovery at production and injection wells, respectively, when injection is stopped after one, two, or five years. Recovery at the injection well is relatively more rapid, because temperature gradients in the rock are larger near the injection point, and because a buoyancy-driven convection cell develops in the fracture. The circulation pattern is counterclockwise in Figure 5, removing cold fluid from the vicinity of the injection point. This effect decreases the rate of temperature recovery at the production well, but significant recovery occurs

nonetheless in a period of a few months. This is encouraging in the sense that shutting-in an injection well appears to be a viable cure if thermal interference has caused unacceptable temperature decline in a production well which is connected with an injection well by a preferential flow path. Thermal recovery has been observed in several fields. For example, Wairakei well WK107 produced again at its original temperature after 300 tonnes/hour of 160°C water had been injected for a period of four years (Horne, 1982b).

CONCLUSIONS

(1) A reliable determination of the thermal properties of preferential flow paths requires non-isothermal injection over periods of months or years, with careful monitoring of production temperatures.

(2) Rapid tracer breakthrough and large cumulative returns indicate a "preferential flow path", but do not necessarily indicate a potential for rapid thermal interference.

(3) Predictions of thermal interference can be made on the basis of tracer data alone. However, this will usually require an ad hoc model for the flow path geometry, and the reliability of thermal predictions on this basis is uncertain.

(4) If thermal interference along a preferential flow path causes unacceptable declines in production temperature, shutting-in of the injection well involved should provide an acceptable cure, with substantial temperature recovery to be expected within typically a few months.

NOMENCLATURE

c	specific heat (J/kg °C)
c_1	average specific heat of rock and fluid in fracture (J/kg °C)
c_2	specific heat of rock matrix (J/kg °C)
c_w	specific heat of water (J/kg °C)
C_f	compressibility of fracture (Pa^{-1})
C_r	compressibility of rock (Pa^{-1})
D	molecular diffusivity of tracer, m^2/s
h	reservoir thickness (m)
H	height of vertical fracture (m)
k	permeability (m^2)
L	length of vertical fracture (m)
N_{Pe}	Peclet number
q	flow rate (kg/s)
q_D	dimensionless flow rate in fracture
q_v	volumetric flow rate (m^3/s)
r	radial distance (m)
r_D	dimensionless radial distance, r/w
S	surface area (m^2)
t	time (s)
t_b	fluid residence time (s)
t^*	partial thermal breakthrough time when neglecting heat transfer across fracture faces (s)
t_f	thermal breakthrough time in fracture (s)
t_{f2}	partial thermal breakthrough time from heat transfer across fracture faces (s)
T	temperature (°C)
T_o	initial temperature (°C)
T_f	temperature in fracture (°C)
T_{in}	injection temperature (°C)
v	velocity (m/s)
v_w	pore velocity of water (m/s)
V	volume (m^3)
w	fracture aperture (m)
x	linear distance (m)
x_D	dimensionless distance x/w
x_f	distance from injection point in fracture (m)

Greek

α	group of thermal parameters, defined in Equation (7)
ζ	argument of complementary error function
ξ	dimensionless time-distance parameter
ϕ	porosity
λ	thermal conductivity (W/m °C)
λ_2	thermal conductivity of rock matrix (W/m °C)
ρ	density (kg/m^3)
ρ_1	average density of rock and fluid in fracture (kg/m^3)
ρ_2	density of rock matrix (kg/m^3)
τ	fractional cumulative recovery of tracer
θ	dimensionless parameter in pressure solution, equation (A.1) ($\theta = \phi_r C_r k_r / \phi_f C_f k_f$)
μ	viscosity (Pa · s)

Subscripts

f	fracture
r	rock
w	water

ACKNOWLEDGEMENTS

The authors are indebted to Peter Fuller for valuable help with the calculations. We also thank Drs. P. A. Witherspoon and M. Lippmann for a critical review of the manuscript.

This work was supported by the Assistant Secretary for Conservation and Renewable Energy, Office of Renewable Energy, Division of Geothermal Energy and Hydropower Technologies of the U. S. Department of Energy under Contract No. DE-AC03-76SF00098.

REFERENCES

Bodvarsson, G., "Thermal Problems in the Siting of Reinjection Wells," Geothermics, vol. 1, no. 2, pp. 63-66, 1972.

Bodvarsson, G., "Estimates of Geothermal Resources of Iceland", Proceedings Second United Nations Symposium on the Development and Use of Geothermal Resources, San Francisco, CA, USA, May 20-29, 1975, pp. 33-36.

Bodvarsson, G.S., Pruess, K., and O'Sullivan, M.J., "Injection and Energy Recovery in Fractured Geothermal Reservoirs", paper SPE-11689, presented at the California Regional Meeting of the SPE, Ventura, CA, March 1983.

Bodvarsson, G.S., and Tsang, C.F., "Injection and Thermal Breakthrough in Fractured Geothermal Reservoirs", Journal of Geophysical Research, vol. 87, no. B2, pp. 1031-1048, February 1982.

Coats, K. H., and Smith, B.D., "Dead-end Pore Volume and Dispersion in Porous Media", Society of Petroleum Engineers Journal, pp. 73-84, March 1964.

Dash, Z.V., Murphy, H.D., and Cremer, G.M., "Hot Dry Rock Geothermal Testing: 1978 to 1980", Los Alamos National Laboratory, report LA-9080-SR, Los Alamos, NM, November 1981.

Earlougher, Jr., R.C., "Advances in Well Test Analysis", Society of Petroleum Engineers, Monograph 5, 1977.

Fossum, M.P., and Horne, R.N., "Interpretation of Tracer Return Profiles at Wairakei Geothermal Field Using Fracture Analysis", Transactions, Geothermal Resources Council, vol. 6, pp. 261-264, October 1982.

Fridleifsson, I.B., "Lithology and Structure of Geothermal Reservoir Rocks in Iceland", Proceedings Second United Nations Symposium on the Development and Use of Geothermal Resources, San Francisco, CA, USA, May 20-29, 1975, pp. 371-376.

Grant, M.A. and Garg, S.K., "Baca Geothermal Demonstration Project; Interpretation of Downhole Data from the Baca Geothermal Field", Systems Science and Software (S-Cubed), La Jolla, California, 1981.

Gringarten, A.C., and Sauty, J.P., "A Theoretical Study of Heat Extraction From Aquifers with Uniform Regional Flow", J. of Geoph. Res., vol. 80, no. 35, pp. 4956-4962, 1975.

Hanson, J.M., and Kasameyer, P.W., "Predicting Production Temperature Using Tracer Methods", Transactions, Geothermal Resources Council, vol. 2, pp. 257-258, 1978.

Hantush, M.S., "Modification of the Theory of Leaky Aquifers", J. of Geoph. Res., vol. 56, p. 3713, 1960.

Hayashi, M., Mimura, T., and Yamasaki, T., "Geological Setting of Reinjection Wells in the Otake and Hatchobaru Geothermal Field, Japan", Transactions, Geothermal Resources Council, vol. 2, pp. 263-266, 1978.

Horne, R.N., and Rodriguez, F., "Dispersion in Tracer Flow in Fractured Geothermal Systems", Proc. Seventh Workshop Geothermal Reservoir Engineering, Stanford University, Stanford, CA, pp. 103-107, December 1981.

Horne, R., "Geothermal Reinjection Experience in Japan", J. Petr. Techn., pp. 495-503, March 1982a.

Horne, R., "Effects of Water Injection into Fractured Geothermal Reservoirs - A Summary of Experience Worldwide", Geothermal Resources Council, Special Report No. 12, pp. 47-63, August 1982b.

Lauwerier, H.A., "The Transport of Heat in an Oil Layer Caused by the Injection of Hot Fluid", Appl. Sci. Res., Martinus Nijhoff, Publisher, The Hague, vol. 5, section A., no. 2-3, pp. 145-150, 1955.

Murphy, H.D., and Tester, J.W., "Heat Production From a Geothermal Reservoir Formed by Hydraulic Fracturing - Comparison of Field and Theoretical Results", paper SPE-8265, presented at the Society of Petroleum Engineers 54th Annual Fall Technical Conference and Exhibition, Las Vegas, NV, September 1979.

Murphy, H.D., Tester, J.W., Grigsby, C.O., and Potter, R.M., "Energy Extraction From Fractured Geothermal Reservoirs in Low-Permeability Crystalline Rock", J. of Geoph. Res., vol. 86, no. B8, pp. 7145-7158, August 1981.

Pruess, K. and Narasimhan, T.N., "A Practical Method for Modeling Fluid and Heat Flow in Fractured Porous Media", Proc. Sixth SPE-Symposium on Reservoir Simulation (paper SPE-10509), New Orleans, LA, February 1982.

Pruess, K., "Development of the General Purpose Simulator MULKOM", Annual Report 1982, Earth Sciences Division, Lawrence Berkeley Laboratory, to be published 1983.

Raghavan, R., "Pressure Behavior of Wells Intercepting Fractures", Proc. 1st Invitational Well-Testing Symposium, LBL-7027, Lawrence Berkeley Laboratory, Berkeley, CA, October 19-21, 1977.

Robinson, B.A., "Quartz Dissolution and Silica Deposition in Hot Dry Rock Geothermal Systems", Los Alamos National Laboratory, report LA-9404-T, Los Alamos, NM, 1982.

Stehfest, H., "Numerical Inversion of Laplace Transforms", Communications ACM, vol. 13, pp. 44-49, 1970.

Tester, J.W., Bivins, R.L., and Potter, R.M., "Interwell Tracer Analysis of a Hydraulically Fractured Granitic Geothermal Reservoir", Society of Petr. Eng. J., pp. 537-554, August 1982.

Vinsome, P.K.W., and Westerveld, J., "A Simple Method For Predicting Cap and Base Rock Heat Losses in Thermal Reservoir Simulators", J. Canadian Petroleum Technology, pp. 87-90, July-September 1980.

Witherspoon, P.A., Wang, J.S.Y., Iwai, K., and Gale, J.E., "Validity of Cubic Law for Fluid Flow in a Deformable Rock Fracture", Water Resources Research 16(6), pp. 1016-1024, 1980.

Zyvoloski, G., (ed.), "Evaluation of the Second Hot Dry Rock Geothermal Energy Reservoir: Results of Phase I, Run Segment 5", Los Alamos National Laboratory, report LA-8940-HDR, Los Alamos, NM, August 1981.

APPENDIX

Here we will give solutions for the dimensionless flow rate in vertical and horizontal fractures as a function of dimensionless time and distance. One-dimensional flow in the rock matrix is assumed for both cases. These solutions can be found in the groundwater and petroleum literature. The solutions are given in the Laplace domain, and are inverted numerically using an inverter developed by Stehfest (1970).

Vertical Fracture (constant rate)

In the Laplace domain the solution for the dimensionless pressure is:

$$u = \frac{1}{p\sqrt{z}} \exp - [x_D\sqrt{z}] \qquad x_D > 1 . \qquad (A.1)$$

where $z = p + \sqrt{\theta p}$, p being the Laplace parameter. The dimensionless flowrate along the fracture can be obtained by differentiating equation (A.1) w.r.t. x_D:

$$\frac{\partial u}{\partial x_D} = - \frac{1}{p} \exp - [x_D\sqrt{z}] \qquad (A.2)$$

Horizontal Fracture (constant rate)

In the Laplace domain the dimensionless pressure in the fracture is:

$$u = \frac{1}{p} K_o(r_D\sqrt{z}) \qquad (A.3)$$

where K_o is the modified Bessel function of zero order. Equation (A.3) has been inverted to real space by Hantush (1960). The dimensionless flowrate is:

$$\frac{\partial u}{\partial r_D} = \frac{\sqrt{z}}{p} K_1(r_D\sqrt{z}) \qquad (A.4)$$

Equations (A.2) and (A.4) have been inverted numerically to yield the fractional flow rate q_D in the fracture, (see Table II and Figure 3).

TABLE I

SELECTED TRACER DATA FROM GEOTHERMAL FIELDS WITH PREFERENTIAL FLOW PATHS
(compiled from Horne, 1982 a,b; Fossum and Horne, 1982; Hayashi et al., 1978)

geothermal field	injection well	production or observation well	injection rate (kg/s)	distance of tracer recovery (m)	average linear velocity (m/hour)	cumulative recovery (%)
Wairakei	WK80	WK116		500	2.7	
		WK76		145	0.7	
		WK108		230	1.1	
	WK107	WK24			22	3.7
		WK48			7.0	1.3
	WK101	WK121		500	8.0	6.0
		WK103			1.3	
		WK116			2.0	
Ohaaki (Broadlands)	BR13	BR23	41.7	270	0.4	6.0
	BR28	BR25	41.7		0.8	
	BR33	BR11	83.3	75	0.4	12.0
		BR8				5.0
Hatchobaru	HR17	H7	97.2		78.0	
		H3			16.0	
	H6	H14	11.1		35.0	
		H4			8.0	
		H13			2.0	
	H-9R	H13	19.4		62.0	
	H3	H4		140	6.1	
		H6		135	33.8	
		H7		180	9.0	
Otake	OR-2	O-8		125	0.2	
		O-9		203	0.3	
		O-10		140	0.2	
Tongonan	4R1	404		≈400	57.0	11.5
		401		≈200	30.0	2.8
		108		≈200	22.0	2.0

TABLE II

FRACTIONAL FLOW RATE ALONG FRACTURE

x_r (m)	$k_f w$ (m^3)	k_r (m^2)	q_D vertical fracture	q_D horizontal fracture
250	10^{-10}	10^{-17}	.995	1.0
250	10^{-10}	10^{-15}	.78	.999
250	10^{-12}	10^{-17}	.98	.995
250	10^{-12}	10^{-15}	.94	.992
250	10^{-14}	10^{-17}	.485	.73
250	10^{-14}	10^{-15}	.08	.19
1000	10^{-10}	10^{-17}	.97	.995
1000	10^{-10}	10^{-15}	.92	.990
1000	10^{-12}	10^{-17}	.922	.991
1000	10^{-12}	10^{-15}	.763	.935
1000	10^{-14}	10^{-17}	.04	.11
1000	10^{-14}	10^{-15}	.0	.0

(Parameters: ϕ_r = .1, C_r = $10^{-9}Pa^{-1}$, t = 1 year, μ = $10^{-4}Pa\cdot s$)

TABLE III

PARAMETERS USED IN THE VERTICAL FRACTURE INJECTION SIMULATION

Rock	
Heat conductivity	2.1 W/m°C
Volumetric specific heat	2.65×10^6 J.m^3°C
Permeability	0
Fracture	
Height	200 m, 400 m
Length	240 m
Aperture	.01 m, .04 m
Porosity	50%
Permeability	50, 200, 500 darcy
Initial Conditions	
Temperature	300°C
Pressure	hydrostatic profile with P_{av} = 100 bar
Injection	
Temperature	100°C
Rate	4 kg/s
Production	
Productivity index of production well	4×10^{-12} m^3
Flowing bottomhole pressure	9.56 MPa

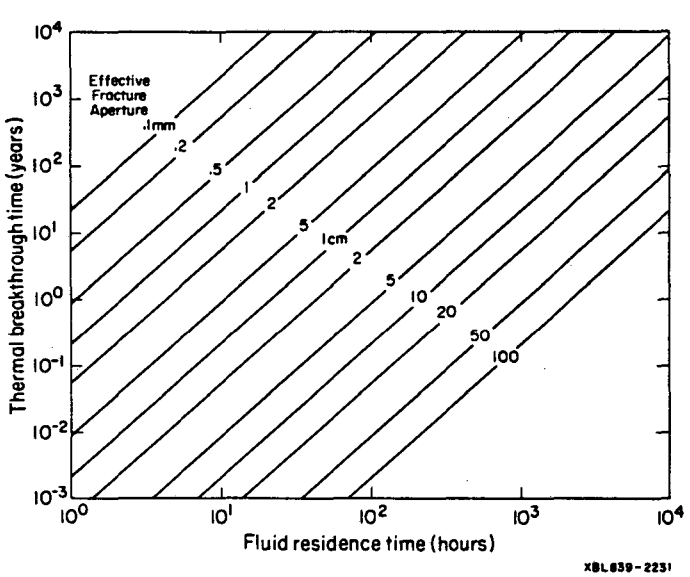

Fig. 1. Thermal breakthrough time as function of fluid residence time and effective fracture aperture (from Equation 9).

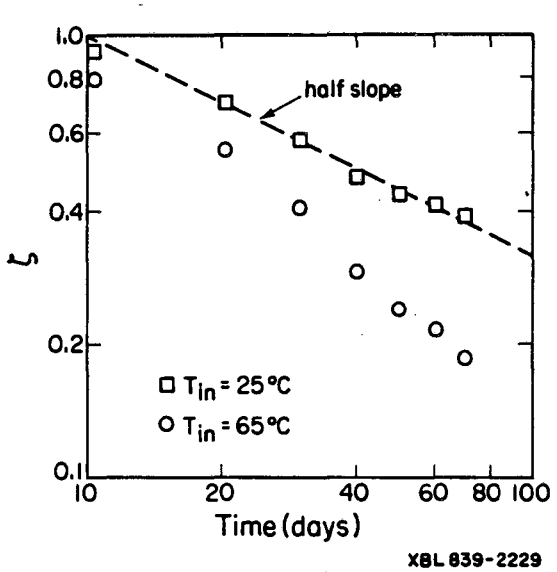

Fig. 2. Temperature decline in the Los Alamos hot dry rock experiment, run segment 2. (The parameter ζ is defined in Equation 11.)

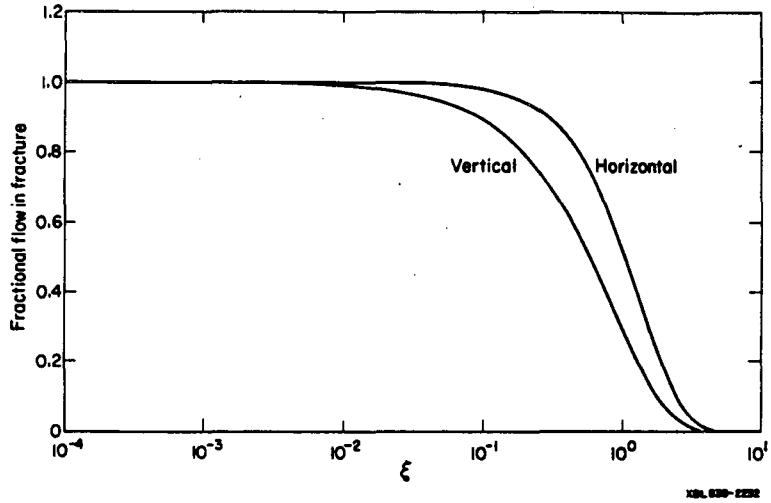

Fig. 3. Fractional flow rate in fracture versus distance, for a case with permeable rock matrix.

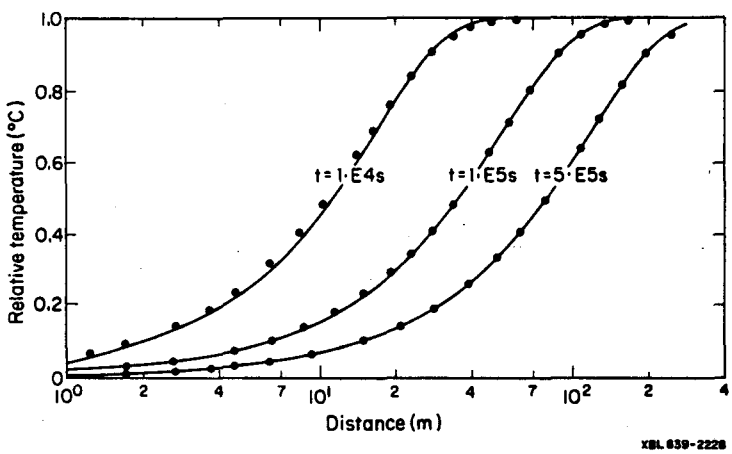

Fig. 4. Comparison of analytical (solid lines) and numerical results for thermal fronts in one-dimensional fracture flow.

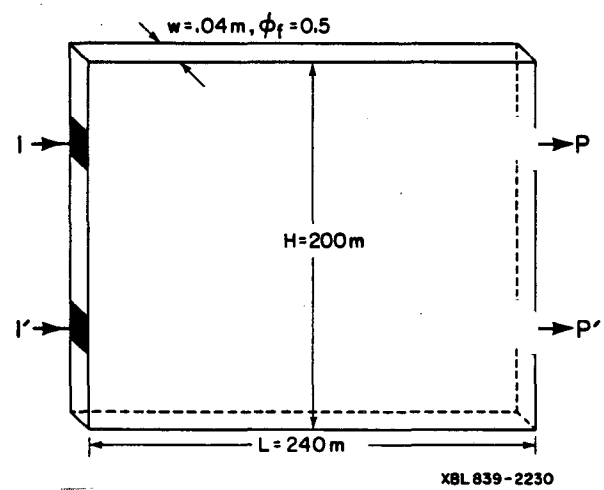

Fig. 5. Schematic diagram of injection-production system in vertical fracture. (I, I' - injection points; P, P' - production points.

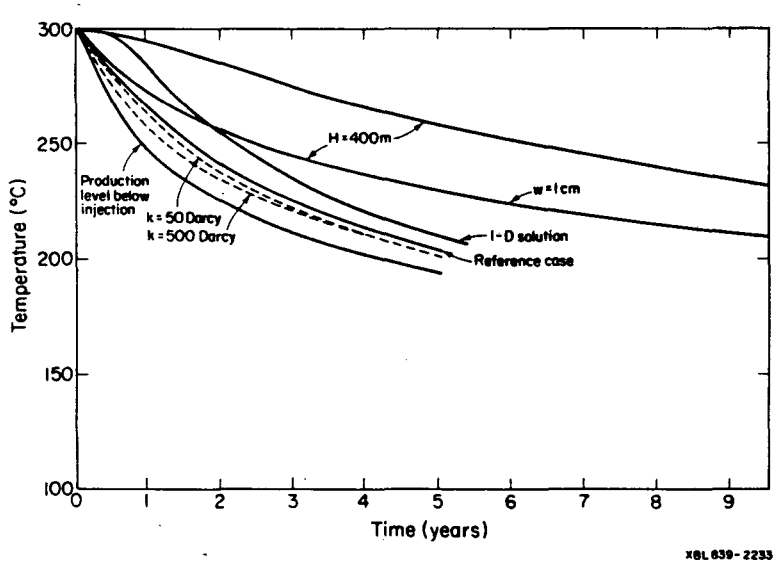

Fig. 6. Simulated production temperatures for injection-production systems in vertical fractures. Reference fracture parameters are H = 200 m, L = 240 m, w = .04 m, ϕ_f = 50%, k_f = 200 x 10^{-12} m^2.

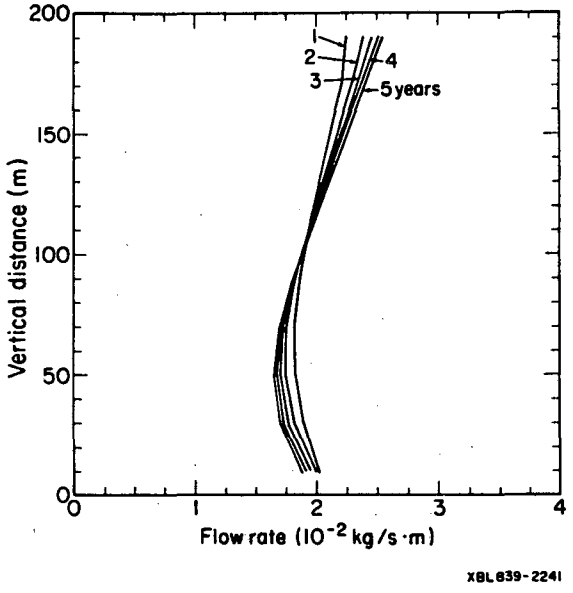

Fig. 7. Horizontal flow rate through a vertical plane at fracture center (between injection and production points) for permeability $k_f = 50 \times 10^{-12}$ m^2.

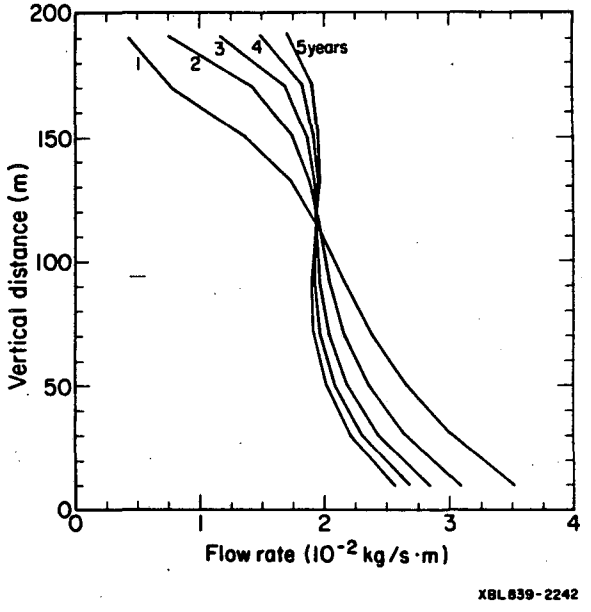

Fig. 8. Same as Figure 7, but $k_f = 200 \times 10^{-12}$ m^2.

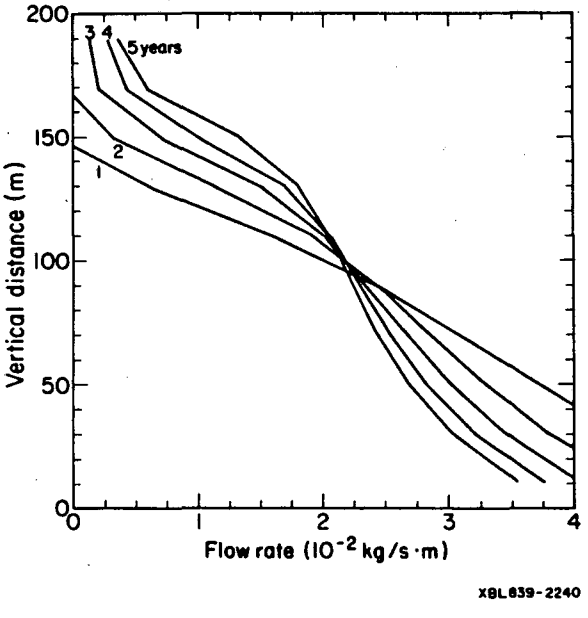

Fig. 9. Same as Figure 7, but $k_f = 500 \times 10^{-12}$ m^2.

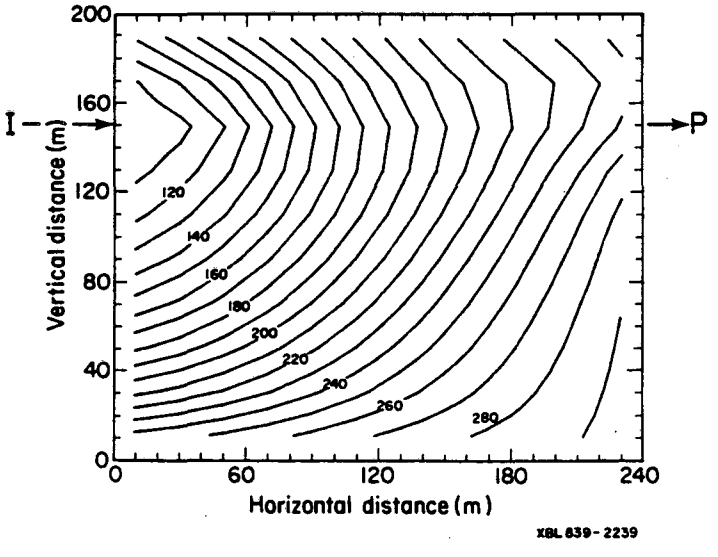

Fig. 10. Temperature contours in fracture plane after one year of production and injection. Permeability $k_f = 50 \times 10^{-12}$ m^2.

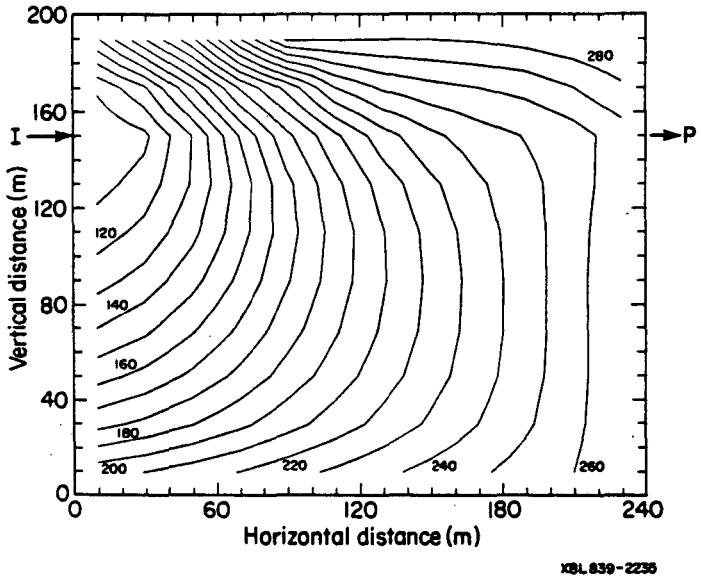

Fig. 11. Same as Figure 10, but $k_f = 200 \times 10^{-12}$ m^2.

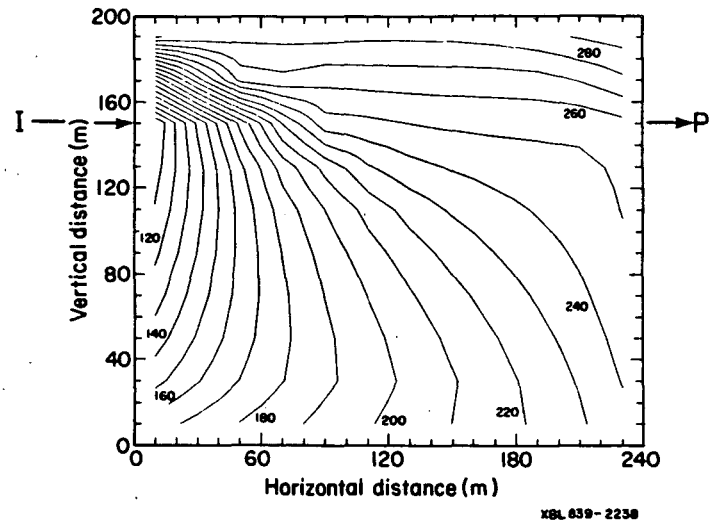

Fig. 12. Same as Figure 10, but $k_f = 500 \times 10^{-12}$ m^2.

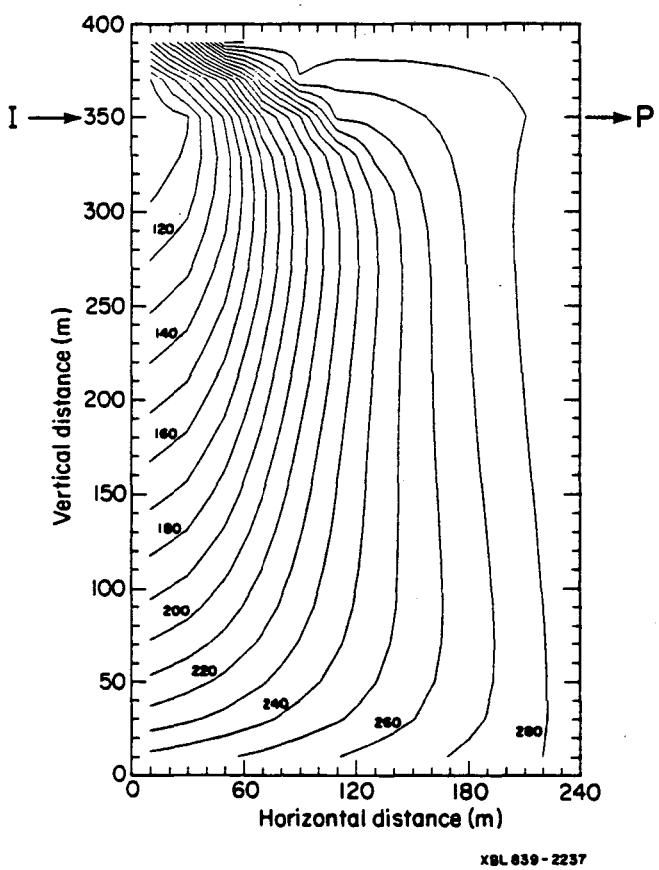

Fig. 13. Temperature contours in fracture plane after two years of production and injection, for a fracture of height H = 400 m, permeability $k_f = 200 \times 10^{-12}$ m^2.

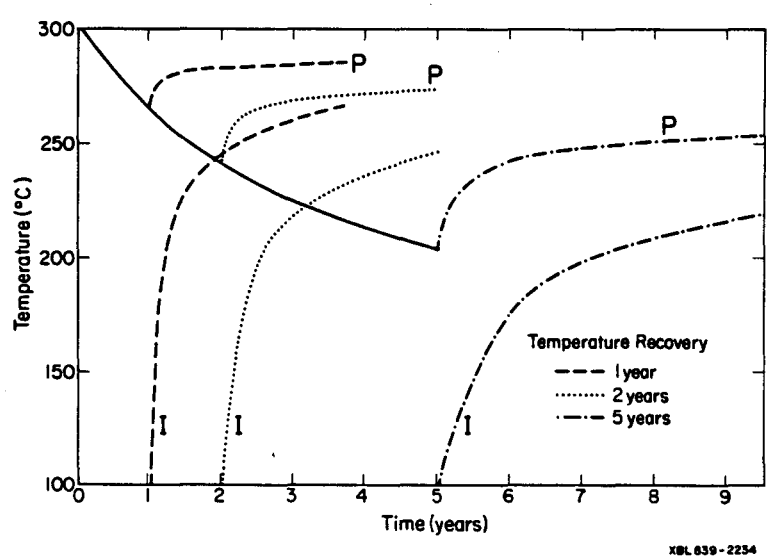

Fig. 14. Temperature recovery at production and injection points (P and I, respectively), when injection is stopped after different time periods. Parameters are for the reference case, see Figure 6.

This report was done with support from the Department of Energy. Any conclusions or opinions expressed in this report represent solely those of the author(s) and not necessarily those of The Regents of the University of California, the Lawrence Berkeley Laboratory or the Department of Energy.

Reference to a company or product name does not imply approval or recommendation of the product by the University of California or the U.S. Department of Energy to the exclusion of others that may be suitable.

TECHNICAL INFORMATION DEPARTMENT
LAWRENCE BERKELEY LABORATORY
UNIVERSITY OF CALIFORNIA
BERKELEY, CALIFORNIA 94720